Photocatalytic decolorization of methylene blue by an immobilized TiO_2 film under visible light irradiation: optimization using response surface methodology (RSM)

Ali H. Jawad[a,b,*], Abbas F.M. Alkarkhi[c], Nur Shazwani Abdul Mubarak[a]

[a]*Faculty of Applied Sciences, Universiti Teknology MARA (UiTM), 40450 Shah Alam, Selangor, Malaysia,*
emails: ahjm72@yahoo.com (A.H. Jawad), shazwanimubarak@yahoo.com (N.S.A. Mubarak)
[b]*Environment and Biomass Research Laboratory, Universiti Teknologi MARA (UiTM), 02600 Arau, Perlis, Malaysia*
[c]*Division of Environmental Technology, School of Industrial Technology, Universiti Sains Malaysia, 11800 Minden, Penang,*
Malaysia, email: abbas@usm.my

ABSTRACT

In this study, response surface methodology, based on face-centered composite design was used to investigate the effect of operational parameters on the decolorization of methylene blue (MB) using an immobilized film of TiO_2 onto glass plate under a 55-W household fluorescent lamp irradiation. Three operating variables, namely TiO_2 loading (0.65–3.9 mg/cm^2), pH (2–10), and irradiation time (15–90 min) with a total of 20 individual experiments conducted to optimize the combination effects of the variable. The significance of the model and regression coefficients was tested by the analysis of variance. Analysis of the data obtained showed there was a strong significant influence of the operational factors and their interactions on MB color removal ($p < 0.0001$) of the photocatalytic decolorization process. The results predicted by the models were found to be in good agreement with those obtained by performing experiment ($R^2 = 0.9706$ and Adj-$R^2 = 0.9442$). For MB color removal, the photocatalytic decolorization process was significantly influenced by the pH and irradiation time, whereas the TiO_2 loading shows less effect. The optimum TiO_2 loading, pH, and irradiation time were found to be 3.06 mg/cm^2 (thickness = 42.43 ± 1.15 μm), 8.25 and 89.76 min, respectively. Under optimum conditions, high photocatalytic efficiency for MB color removal, 98.01% was observed. The kinetics of MB decolorization at optimum conditions was well fitted to the pesudo-first-order kinetic model.

Keywords: Photocatalyst; TiO_2; Basic dye; Visible light; Optimization; Modeling

1. Introduction

In the present days, huge amounts of colored wastewater are generated in industries, which, basically, utilize dyes to impart a demanded color to their products such as plastic, rubber, textile, wood, paper, and food. The existing of dyes in natural streams is not only esthetically unpleasant but also can cause serious problem to the ecosystem by increasing toxicity, and level of chemical oxygen demand and retardation of photosynthesis phenomena by reducing penetration of light [1]. Among the various types of

*Corresponding author.

dyes, various cationic dyes, methylene blue (MB) is the most frequently used cationic dye for dyeing silk, wood, paper, cotton, wool, and temporary hair colorant. The extensive usage of MB can often cause eye burns, which may be a main reason for permanent injury to the eyes of mankind and animals. In this respect, MB inhalation can give rise to short periods of rapid or difficult breathing, while ingestion through the mouth produces a burning feeling and may lead to vomiting, methemoglobinemia, nausea, and mental confusion [2,3]. MB has a complicated chemical structure; it is not easy to be removed from wastewaters by conventional used techniques such as biological treatment and chemical precipitation. Therefore, many other effective methods like adsorption, electrocoagulation, ultrasonic decomposition, advanced chemical oxidation, nanofiltration, and chemical coagulation followed by sedimentation were used to protect the aquatic environment by removing dyes from wastewater [4,5].

In recent years, advanced oxidation processes (AOPs) have attracted remarkable attention for the treatment of effluents containing refractory compounds [6]. The principle of AOPs is based on *in situ* generation of highly reactive radical species, which are capable of degrading the pollutants by the use of solar, chemical, or other forms of energy. In fact, the photocatalytic oxidation process is a surface phenomenon and all photoreactions take place at the surface of a semiconductor catalyst such as titanium dioxide [7]. Among all of the semiconductor photocatalysts, titanium dioxide, up to, now stands to be an ideal bench mark photocatalyst in the environmental photocatalysis applications because of its many desirable properties such as inexpensive and readily available, biologically and chemically inert, and good photoactivity compare to other semiconductors [8]. In addition, it has the ability for degrading organic pollutants present at or close to the TiO_2 surface, resulting in their complete mineralization into H_2O and CO_2 [9].

However, there are two major technical challenges that remarkably limited its potential field applications. First, the relatively wide band gap of TiO_2, which is absorbed only by 3–4% energy of the solar spectrum and restricted its applications to UV excitation source [10]. Second, the effective slurry or suspension mode application of TiO_2 needs post-treatment catalyst recovering step, which is normally difficult, energy consumptive, and not cost effective. Moreover, the TiO_2 powder has a great tendency to aggregate, especially at high concentrations, which provides a real limitation to apply to continuous flow system and suffers from scattering of incident UV light by the suspended particles [11,12].

Optimizing refers to improving the performance of the applied system, a process, or a product in order to achieve the maximum benefit from it. The term optimization has been commonly used in unlimited chemistry applications as a means of investigating conditions at which, to apply a procedure that produces the optimum possible response [13]. Generally, optimization in chemistry applications had been performed by monitoring the effect of one factor at a time on an experimental response. While only one parameter is changed, others are fixed at a certain level. This optimization technique is called one-variable-at-a-time. Its main disadvantage is that it does not take into account the interactive effects among the variables studied. As a result, this technique does not depict the complete effects of the parameter on the response [14]. Another disadvantage of the one-factor optimization is the increase in the number of experiments necessary to conduct the research, which result in increasing of time, labor, expenses in addition to an increase in the consumption of chemicals, reagents, and materials [15,16]. For solving this problem, the optimization of experimental procedures had been carried out using multivariate statistic techniques. Among the most relevant multivariate techniques used in variable optimization, is the response surface methodology (RSM).

RSM is a powerful tool used for reducing the number of experimental runs needed to provide sufficient information for statistically acceptable results. Thus, it is less laborious and time consuming compared with the full factorial experimentation. Response surface procedures are primarily used for discovering a set of process variables which are most important to the process and then determine at what levels these factors must be kept to obtain an optimum performance [17].

In very recent years, only few works are concerning the mathematical modeling of the photodegradation and photocatalytic degradation of organic pollutants and textile effluents under various light sources using unmodified and modified TiO_2 in aqueous suspension [8,15–19]. Therefore, the purpose of this work was to apply the RSM for identifying the optimum operation conditions for the photocatalytic decolorization of MB in batch photo-reactor using an immobilized TiO_2 film onto glass plate under visible light (55-W fluorescent household lamp). The experimental work was performed using face-centered composite design (FCCD) to determine the main effects and the interaction between TiO_2 loading onto glass plate, pH, and irradiation time. In fact, the photocatalysis is a surface phenomenon requiring direct contact between the MB and the catalyst surface. Thus, the electrostatic interaction between photocatalyst surface, MB molecules, and charged radicals formed during

photocatalytic decolorization as well as protonation and deprotonation of organic pollutants are basically dependent on the pH of the solution and catalyst surfaces property. Therefore, TiO_2 loading on solid support and pH of solution were chosen as the crucial variables in this study in addition to the irradiation time.

2. Materials and methods

2.1. Materials

Titanium (IV) oxide (99% anatase) powder of particle size $\leq 150\,\mu m$ was obtained from Sigma–Aldrich. Epoxidized natural rubber (ENR50) was obtained from Kumpulan Guthrie Sdn. Bhd., Malaysia. Toluene and acetone were purchased from BDH analar. Hydrochloric acid (HCl) obtained from R & M Chemicals and sodium hydroxide (NaOH) pellets purchased from Mallinkoot were used adjusting pH. MB dye (c.a. 98%, Color Index Number: 52015), was purchased from R & M. Table 1 summarizes chemical structure, molecular weight, and λ_{max} for MB. All the materials were used as received without further purification. Ultrapure water ($18.2\,M\Omega\,cm^{-1}$) was used to prepare all solutions in this study. Chemicals used in this experiment were all of analytical grades and used without further purification of modification.

2.2. Preparation of TiO_2 formulation

The TiO_2 photocatalyst formulation was obtained by adding a fixed amount of 5 g ENR50 solution (11.32% solution of ENR50 in toluene) into an amber bottle, which contained 12 g TiO_2 powder. After that, 60 mL of acetone was poured into the bottle before being homogenized by sonication process for 5 h using ultrasonic cleaner set, model WUC-D06H (50–60 Hz) from Daihan scientific Co. Ltd. A simple dip-coating method was used to immobilize TiO_2 formulation onto glass plate. Glass plates with smooth surfaces on one side with dimensions 47 mm (width) × 70 mm (height)

were used as an inert solid support materials for immobilizing the photocatalyst formulation. The varying amounts of TiO_2 photocatalyst was produced by dipping and drying a glass plate at varying number of times in the TiO_2 formulation. In the dip-coating method, it was found that the catalyst loading was directly proportional to the number of dips into the TiO_2 formulation. Scanning electron microscopy (SEM, Model Leica Cambridge S360) was used to measure the thickness and also to observe the surface morphology of the immobilized TiO_2 film.
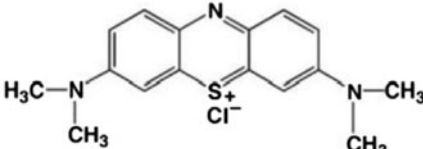
2.3. Photo-reactor and light source

A custom made glass photo-reactor cell with length 58 mm, width 10 mm, and height of 80 mm was used for all the photocatalytic experiments. A compact 55-W fluorescent lamp (Qusun) with UV content of $0.732\,Wm^{-2}$ and visible $441\,Wm^{-2}$ was used as the light source. The UV and visible content in a compact 55-W fluorescent lamp was measured using a radiometer (Solar light Co. PMA 2100) connected with a UV-A and UV-B broadband detector (PMA 2130), and visible light detector (PMA 2132). This lamp was placed vertically in contact with the outer surface of the photo-reactor cell. Twenty mL of $20\,mg\,L^{-1}$ MB solution was poured inside the photo-reactor cell. The initial pH of the MB solution was adjusted by adding either 0.1 M HCl or NaOH until the desired pH value was obtained by monitoring with a Metrohm, 827 pH lab. After that, an immobilized glass/TiO_2 film was placed upright inside the photo-reactor cell and exposed directly to the light source. The aeration flow rate was maintained at $25\,mL\,min^{-1}$ throughout the photocatalytic decolorization process. The schematic diagram of the complete photo-reactor and light source setup is presented in our previous work [20].

2.4. Photocatalytic efficiency and kinetic study

The concentration of degraded MB during the photocatalytic decolorization process was measured

Table 1
Characteristics of MB dye

Chemical structure of MB	Chemical formula	Molecular weight (g mol^{-1})	λ_{max} (nm)
	$C_{16}H_{18}ClN_3S\cdot2H_2O$	319.85	661 nm

for its respective absorbance using a DR 2800 HACH spectrophotometer and the results were converted into its corresponding concentration (*C*). The decolorization efficiency was calculated using the following equation:

$$CR\,(\%) = (C_0 - C_t)/C_0 \times 100 \tag{1}$$

where CR (%) is the percentage of color removal (MB) obtained by photocatalytic decolorization process and C_0 and C_t both in (mg L^{-1}) are, respectively, the initial and remaining concentration of MB in solution at time *t* (min).

The kinetics of the photocatalytic decolorization rate of MB was determined using Langmuir–Hinshelwood kinetics model as given in the following equation:

$$\ln\,(C_0/C_t) = k_{app}\,t \tag{2}$$

The pseudo-first-order rate constant, k_{app} (min^{-1}), was calculated from the slope of ln (C_0/C_t) vs. irradiation time *t*.

2.5. Design of experiment

A FCCD with three factors was used to fit a second-order response surface model. Twenty runs were required to cover all possible combination of factor levels. This design was to optimize the photocatalytic decolorization process of MB. The effect of three experimental variables, namely TiO$_2$ loading (mg/cm^2) (X_1), pH (X_2), and irradiation time (min) (X_3) on the photocatalytic efficiency of MB color removal was investigated. In order to obtain required data, a total of 20 experiments were carried out in this work, including eight experiments at factorial points, six experiments at axial point, and six replications at central points, derived from the following equation [21].

$$N = 2^n + 2n + n_c = 2^3 + 2(3) + 6 = 20 \tag{3}$$

where *N* is the total number of experiments required and *n* is the number of factors.

In this respect, to ease the statistical calculations, the variables (X_i) are being coded as x_i according to the following Eq. (4) [22]:

$$x_i = \frac{X_i - X_0}{\Delta X_i} \tag{4}$$

where X_0 is the value of X_i at the center point and ΔX_i presents the step with maximum and minimum values of variable X_i.

The experimental ranges and the levels (coded and uncoded) of the independent variables that were determined by the preliminary experiments are given in Table 2. The center points were used to determine the experimental error and the reproducibility of the data. The independent variables are coded to the (−1, 1), interval where the low and high levels are coded as −1 and +1, respectively. The axial points are located at (±α, 0, 0), (0, ±α, 0), and (0, 0, ±α), where α is the distance of the axial point from center and makes the face-centered composite design. The α value was fixed at 1.68179 (face centered). The correlation between response variable and independent variable associated with the central composite matrix was approximated by the following the second-order quadratic polynomial Eq. (5) [23]:

$$y = \beta_0 + \sum_{i=1}^{k} \beta_i x_i + \sum_{i=1}^{k} \beta_{ii} x_i^2 + \sum_{i=1}^{k}\sum_{i \neq j=1}^{k} \beta_{ij} x_i x_j + \varepsilon \tag{5}$$

In this equation, *y* is the response (dependent variables), β_0 is the constant coefficient, β_i, β_{ii}, and β_{ij} are the coefficients for the linear, quadratic, and interaction coefficient, χ_i and χ_j are the coded values of the photocatalytic decolorization of MB variables, and ε is the residual term.

2.6. Model fitting and statistical analysis

In this work, the least square method was used for solving Eq. (5) and calculating the model coefficients. This method is a multiple regression technique for fitting a mathematical model to a set of experimental data producing the minimized sum of the squared differences between the actual and the predicted data [24]. Design-Expert software version 6.0.6 (STAT-EASE Inc., Minneapolis, USA) was used for model-fitting steps, data analysis, and evaluation of the statistical significance of the equations.

2.7. Evaluation of the fitted model

The goodness of the fitted second-order polynomial model was evaluated by the coefficient of determination (R^2) and the analysis of variance (ANOVA).

Table 2
Process variables and their experimental levels

Factor code	Name	Units	Range and levels			
			Actual		Coded	
			Low	High	Low	High
X_1	TiO$_2$ loading	mg/cm^2	0.65	3.9	−1.000	1.000
X_2	pH		2.00	10.00	−1.000	1.000
X_3	Irradiation time	min	15	90	−1.000	1.000

2.8. Optimization analysis

The optimum conditions for three variables: TiO$_2$ loading (X_1), pH (X_2), and irradiation time (X_3) were obtained using data from the statistical analysis. Design-Expert searches for a combination of factors that simultaneously satisfy the requirements placed on each of the response and factors.

3. Results and discussion

3.1. Photocatalyst characterization

Fig. 1(a) and (b) shows representative SEM images of the thickness and surface morphology of the TiO$_2$ film at fixed loading of TiO$_2$ 3.06 mg/cm^2, respectively. As can be seen from Fig. 1(a), the loading of 3.06 mg/cm^2 is responsible for producing 42.43 ± 1.15 μm thickness of an immobilized TiO$_2$ film. Fig. 1(b) shows the surface morphology of TiO$_2$ film, which appears as a relatively regular with amorphous surface structure.

3.2. Statistical analysis

The effect of three independent process variables of TiO$_2$ loading, pH, and irradiation time and their individual and interactive impacts on the color removal efficiency (as response) were investigated in this study using the central composite design approach. A quadratic polynomial model was used for developing the mathematical relationship between the response and the independent process variables. The experimental and predicted results for color removal efficiency of MB color at each point obtained for different combinations of selected variables are presented in Table 3. The empirical relationship between the response (color removal efficiency %) and independent process variable is presented by Eq. (6):

$$Y = +82.98 + 3.52X_1 + 15.00X_2 + 21.52X_3 + 5.64{X_1}^2 - 10.97{X_2}^2 - 6.57{X_3}^2 - 10.84X_2X_3$$
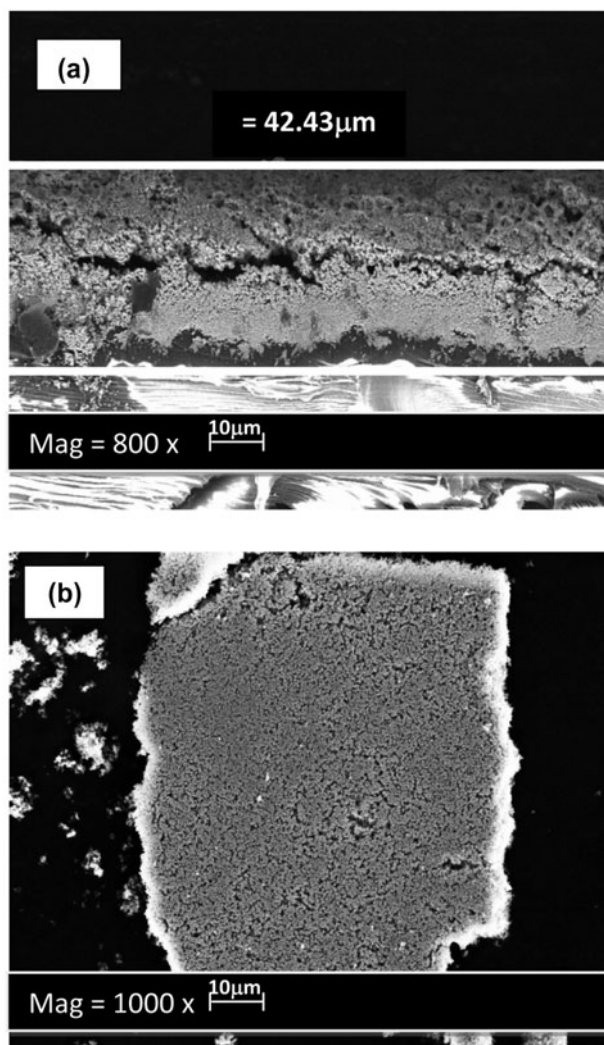
(6)

Fig. 1. (a) A typical SEM micrograph based on the cross-sectional view of the TiO$_2$ film showing the thickness of TiO$_2$ film 42.43 ± 1.15 μm obtained by deposition of 3.06 ± 0.06 mg/cm^2 optimum TiO$_2$ loading onto glass plate, at 800× magnification power and (b) a typical SEM micrograph of the non-irradiated TiO$_2$ film showing the surface morphology of TiO$_2$ photocatalyst, at 1,000× magnification power.

The color removal efficiency (CR%) obtained by photocatalytic decolorization process of MB has been predicted by Eq. (6) and the obtained results are presented in Table 3.

3.3. Model validation

The statistical significance of the CCD model was assessed by ANOVA. The ANOVA results are tabulated in Table 4. The results revealed that the obtained models can be successfully used to navigate the design space. The R^2 values were found to be 0.9706, which is basically close to 1, and advocate a high correlation between experimental and predicted values. This can be observed in Fig. 2 by comparing the experimental values against the predicted responses by the model for the percentage of color removal efficiency of MB. The value of R^2 reveals that 97.06 of the response variability for MB color removal efficiency, is indicated by the model. It implies that, only about 2.94%, the variation for MB color removal efficiency is not explained by the model. Thus, as mentioned previously, in a system with different number of independent variables, adjusted R^2 (Adj-R^2) is more suitable for evaluating the model goodness of fit. In this respect, Adj-R^2 value, 0.9442, was to the corresponding R^2 value. Also, from Table 4, the model F-value of 36.72 reveals that the model is significant. It was also observed that TiO$_2$ loading (X_1) seems does not have a significant effect on the color removal efficiency. On the other hand, the linear term of pH (X_2) has large significant effect on the color removal efficiency due to the high F-value of 84.69. The quadratic term of pH (X_2^2) has also significance with F-value of 12.45. Thus, irradiation time (X_3) also shows a significant effect to the color removal efficiency with F-value of 174.28.

Furthermore, the analysis of the residuals (difference between the observed and the predicted response value) also gives useful information about the model suitability. This analysis consists of identifying the outliers and examining diagnostic plots such as normal probability and residual plots. The normal probability plots show whether the residuals follow a normal distribution, in which case the points will follow a straight line [25]. The plot of normal probability of the residual for MB is depicted in Fig. 3. The trend shown in this figure reveal reasonably well-behaved residual of MB dye and that the residual is normally distributed and resembles a straight line. Moreover, residual vs. predicted response was plotted and presented in Fig. 4. This plot is the residual vs. the ascending predicted response value, which tests the assumption of constant variance. The plot should be a random scatter with a constant range of residuals

Table 3
The 3-factor face-centered composite design matrix and the value of the response function (CR%)

Run	TiO$_2$ loading (mg/cm^2)	pH	Irradiation time (min)	Removal efficiency (%)	
				Actual	Predicted
1	0.65	2	15	18.37	17.91
2	3.9	2	15	30.03	29.49
3	0.65	10	15	69.09	72.23
4	3.9	10	15	76.38	78.57
5	0.65	2	90	87.89	84.57
6	3.9	2	90	96.57	92.30
7	0.65	10	90	96.1	95.51
8	3.9	10	90	98.68	98.01
9	0.65	6	52.5	83.87	85.10
10	3.9	6	52.5	88.85	92.14
11	2.275	2	52.5	48.43	57.01
12	2.275	10	52.5	91.08	87.02
13	2.275	6	15	59.22	54.88
14	2.275	6	90	89.08	97.93
15	2.275	6	52.5	86.22	82.98
16	2.275	6	52.5	84.07	82.98
17	2.275	6	52.5	83.57	82.98
18	2.275	6	52.5	85.42	82.98
19	2.275	6	52.5	84.75	82.98
20	2.275	6	52.5	82.87	82.98

Table 4
ANOVA for quadratic models

Source	Sum of squares	Degree of freedom	Mean square	F-value	p-value
Model	8,784.94	9	976.1	36.72	<0.0001
X_1	123.83	1	123.83	4.66	0.0563
X_2	2,251.2	1	2,251.2	84.69	<0.0001
X_3	4,632.4	1	4,632.4	174.28	<0.0001
X_1^2	87.38	1	87.38	3.29	0.0999
X_2^2	330.83	1	330.83	12.45	0.0055
X_3^2	118.82	1	118.82	4.47	0.0606
X_1X_2	13.7	1	13.7	0.52	0.4892
X_1X_3	7.39	1	7.39	0.28	0.6095
X_2X_3	940.7	1	940.7	35.39	0.0001
Residual	265.81	10	26.58		
Total	9,050.74	19			
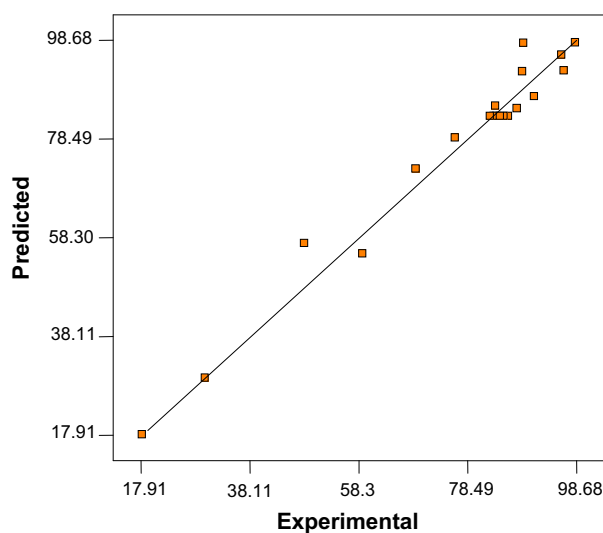
Fig. 2. Comparison of the experimental results of color removal efficiency with the predicted values by FCCD model.

Fig. 3. Normal probability plots for color removal efficiency of MB.

across the graph. Fig. 4 shows that the residuals in the plot fluctuate in a random pattern around the center line.

3.4. Effect of variables

The individual effect of the studied variables, including TiO$_2$ loading (X_1), pH (X_2), and irradiation time (X_3) on the MB color removal efficiency (CR%), was investigated by perturbation plots. The perturbation plot uses the model terms to display the effect of each factor deviation from the reference point on the process response, while holding the other factors c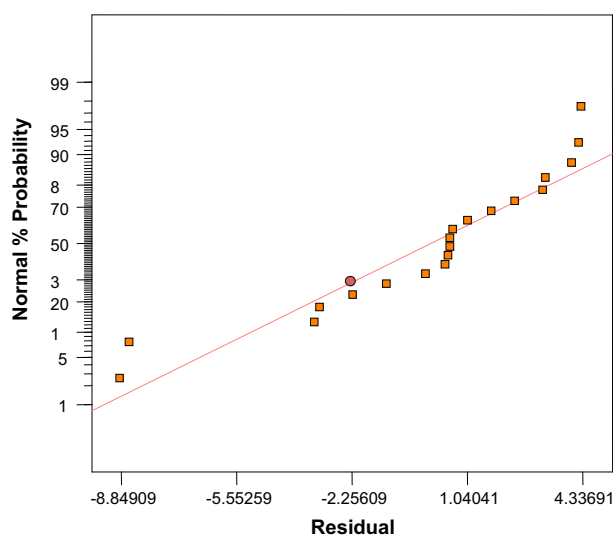onstant. Design-Expert software automatically sets the reference point at the midpoint (coded 0) of all the factors. The perturbation plot can be applied to investigate the most significant factors on the response. A steep slope or curvature in a factor shows that the response is sensitive to that variable. On the other hand, a relatively flat line indicates response insensitivity to change in that particular variable [26]. Perturbation plots for the color removal efficiency of MB are represented in Fig. 5. As can be seen, the TiO$_2$ loading curve shows a slow curvature indicating that this factor has a slight effect on the response. On the other hand, the remarkably steep curvatures in pH and contact time curves indicate that the dye removal efficiency was sensitive to these variables.
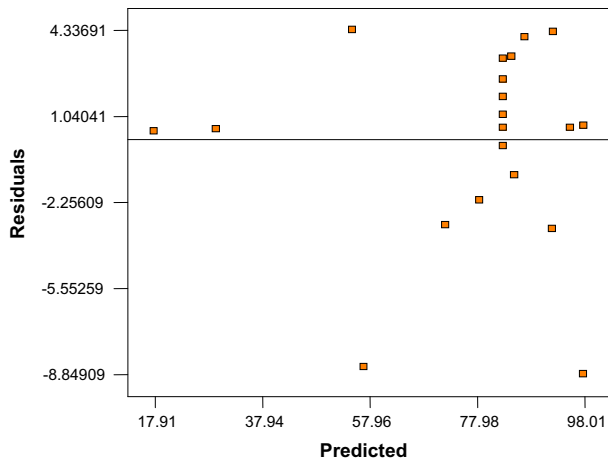
Fig. 4. Residual vs. predicted response values for color removal efficiency of MB.

From same figure, it can be seen that the dye removal efficiency slightly increases as the TiO_2 loading increases, and increases remarkably as pH value moving to moderate basic media, and no significant change can be observed in very strong basic media. Furthermore, the color removal efficiency significantly and directly increases as the irradiation time increases.

To investigate the interaction between all three variables, three-dimensional surfaces and two-dimensional contours were plotted by keeping one variable constant at central level and the other two varying

within the experimental ranges. In Fig. 6, the response surface and contour plots were developed as a function of pH and TiO_2 loading, while the irradiation time was kept constant at 52.5 min. As can be seen in Fig. 6, color removal efficiency increases with an increase in the pH value towards basic environment, while no remarkable changes can be observed by increasing TiO_2 loading. Same behavior can be obtained by plotting the response surface and contour plots of dye removal efficiency as a function of irradiation time and TiO_2 loading, while the pH was kept

(a)

(b)

Fig. 5. Perturbation plots for the color removal efficiency of MB. X_1, TiO_2 loading; X_2, pH; and X_3, irradiation time.
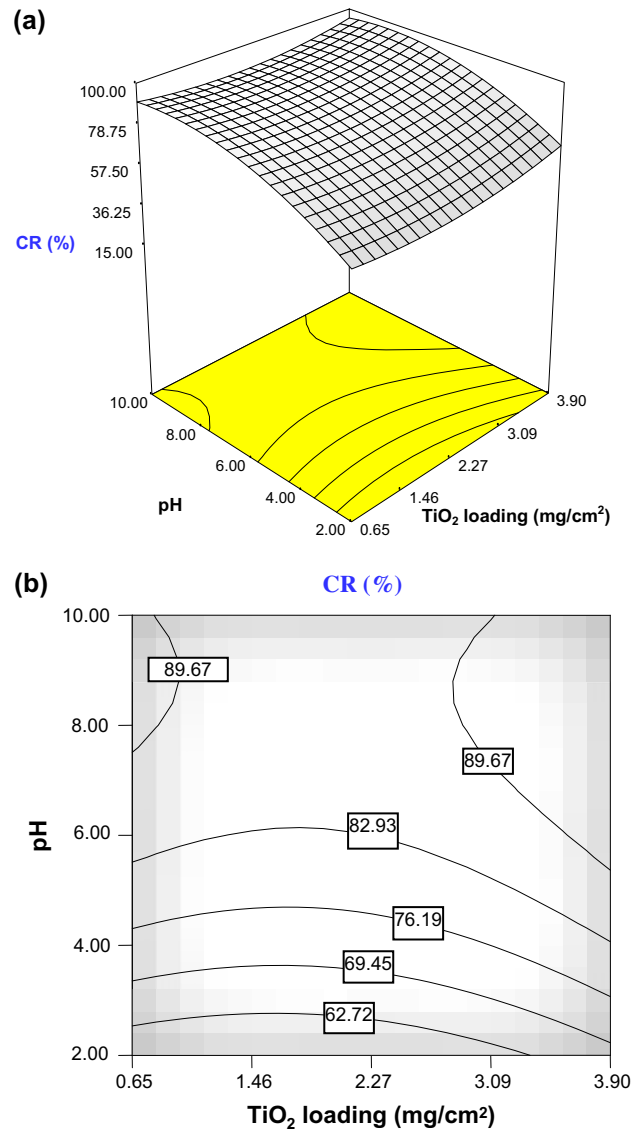
Fig. 6. The response surface (a) and contour plots (b) of the color removal efficiency (CR%) as the function of pH and TiO_2 loading (Irradiation time = 52.50 min and dye initial concentration = 20 mg L^{-1}).

constant at 6, as shown in Fig. 7. As shown in Figs. 6 and 7, the increasing of TiO_2 loading in both cases did not show a significant effect of color removal efficiency. The reason why TiO_2 loading has no remarkable impact on color removal efficiency can be attributed to the limited surface area of the solid support (glass plate), and loading more TiO_2 leads to increase in the thickness of the immobilized catalyst onto the glass plate without significant increase in the number of the photoinduced catalyst particles. Similar

Fig. 7. The response surface (a) and contour plots (b) of the color removal efficiency (CR%) as the function of irradiation time and TiO_2 loading (pH 6 and dye initial concentration = 20 mg L^{-1}).

observation was also reported by Jawad and Nawi [27] in the photocatalytic performances of glass/Chitosan/TiO_2 interface composite film for the degradation of phenol. Therefore, TiO_2 loading was fixed at 2.27 mg/cm^2 during monitoring of the combined effect of pH and irradiation time on the MB color removal efficiency as presented in Fig. 8. It was found from Fig. 8 that the MB color removal efficiency is significantly affected by increasing both pH and irradiation time. Thus, MB color removal efficiency increases with increase in pH value towards a slightly alkaline environment (pH 8) as compared with acidic environment or neutral solution. In fact, the photocatalysis reaction taking place after adsorption process of MB onto photoinduced TiO_2 surface. The adsorption of cationic MB is favored in alkaline solution because when pH is higher than the point of zero charge (Pzc) of the $TiO_2 \approx 6.8$, the TiO_2 surface becomes negatively charged, therefore a higher rate of cationic MB adsorption onto photoinduced TiO_2 surface can be obtained [6].

As for irradiation time, it was also found from Fig. 8 that the color removal efficiency significantly increased with longer exposure time of TiO_2 photocatalyst to the light. In fact, longer exposure time means more generation of hydroxyl radicals, which are responsible for oxidizing the MB dye molecules. In this respect, exposing TiO_2 film to a 55-W fluorescent lamp with UV leakage of 0.732 Wm^{-2} leads to eject the electrons from the valence band (VB) to the conduction band (CB), generating positive holes and free electrons. The absorbed oxygen and molecular water on the surface of TiO_2 film can react with the photogenerated electrons to give O_2^{-}, $HO_2^{•}$, or $^•OH$ as the products Eqs. ((7)–(10)) [28,29].
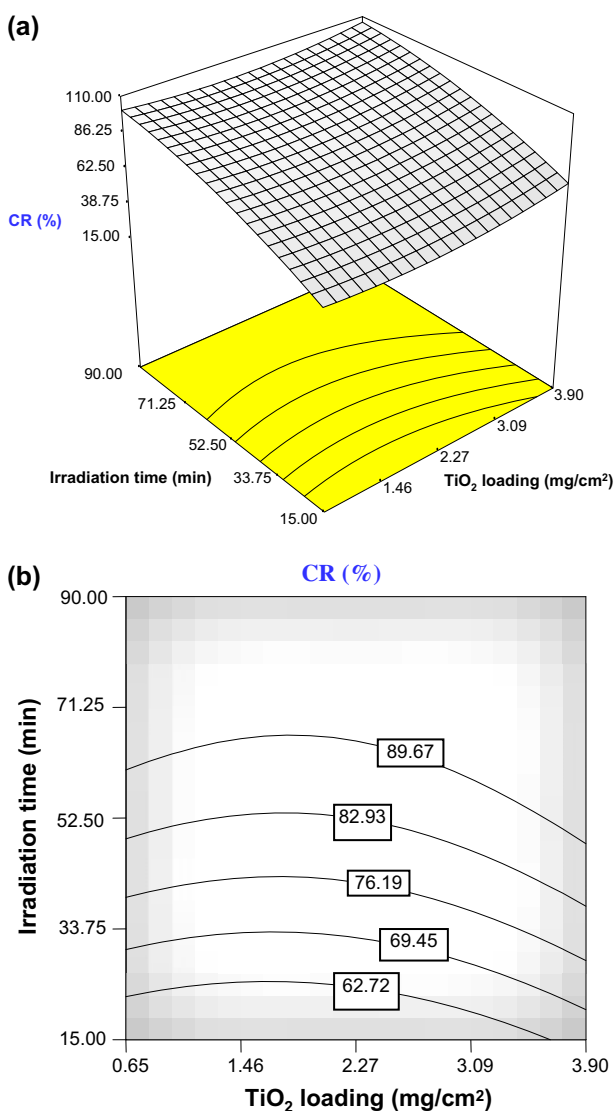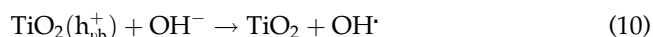
$$TiO_2 + h\upsilon \rightarrow TiO_2\left(e_{cb}^- + h_{\upsilon b}^+\right) \tag{7}$$

$$TiO_2(h_{\upsilon b}^+) + H_2O_{ads} \rightarrow TiO_2 + H^+ + OH^- \tag{8}$$

$$TiO_2(e_{CB}^-) + O_{2ads} \rightarrow TiO_2 + O_{2ads}^- \tag{9}$$

$$TiO_2(h_{\upsilon b}^+) + OH^- \rightarrow TiO_2 + OH^• \tag{10}$$

The $^•OH$ radicals derived from an irradiated TiO_2 surface (Eq. (10)) would directly oxidize MB dye in the bulk solution as in Eq. (11).

$$MB + OH^• \rightarrow oxidation\ products \tag{11}$$
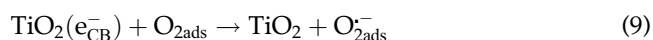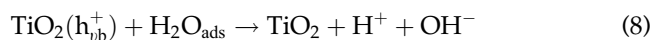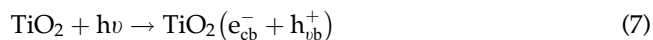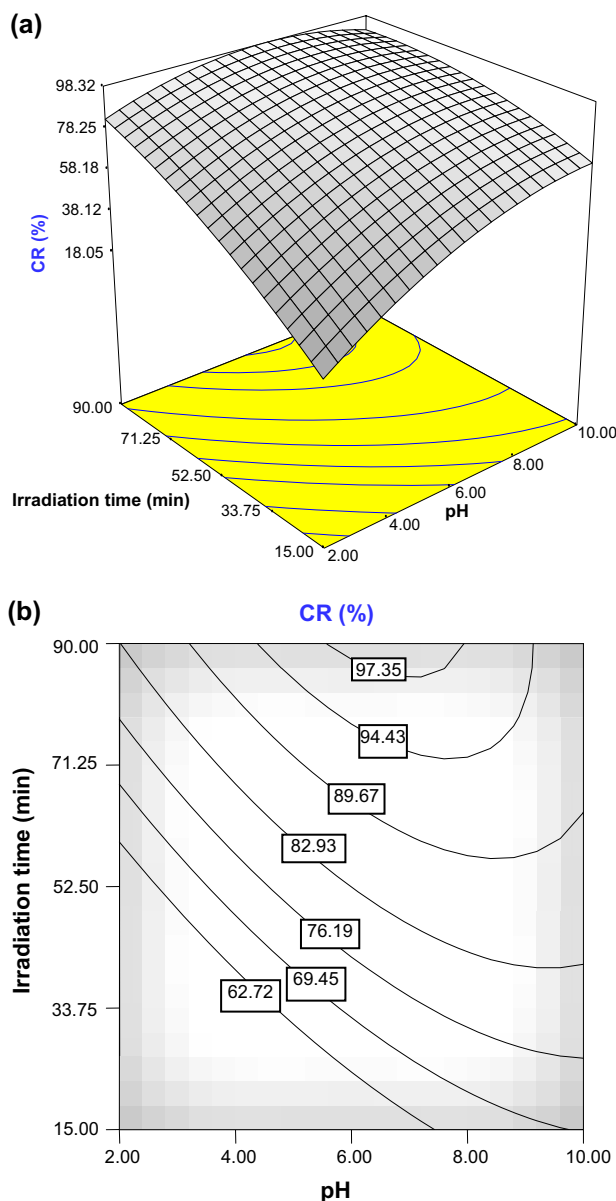
(a)

(b)

Fig. 8. The response surface (a) and contour plots (b) of the color removal efficiency (CR%) as the function of irradiation time and pH (TiO$_2$ loading = 2.27 mg/cm^2 and dye initial concentration = 20 mg L^{-1}).

3.5. Optimization of MB decolorization

To further confirm the model adequacy and verify the optimization results, additional experiments were performed under the predicted optimal conditions and the results are given in Table 5. The experimental values of MB color removal under the optimum conditions were determined as 98.01%. This value is quite comparable to the predicted value, 98.96%, obtained

Table 5
Obtained optimum values of the process variables and response

Variable	Optimum value
TiO$_2$ loading (mg/cm^2)	3.06
pH	8.25
Irradiation time (min)	89.75
MB removal efficiency (%) (predicted)	98.96
MB removal efficiency (%) (experimental)	98.01

from the model and validates the findings of response surface optimization.

3.6. Kinetics of MB decolorization

The kinetics of the photocatalytic decolorization of 20 mL volumes of 20 mg L^{-1} MB under the predicted optimal conditions recorded in Table 5 was determined. The concentration of degraded MB was taken before irradiation ($t = 0$ min) and at every 15 min interval, up to 90 min of irradiation. As shown in Fig. 9, the decolorization efficiency of MB was fitted to the Langmuir–Hinshelwood kinetic model, by plotting ln (C_0/C_t) vs. irradiation time. The obtained linear regression coefficient ($R^2 = 0.971$) was relatively high, indicating that the photocatalytic decolorization of MB obeys the Langmuir–Hinshelwood kinetic model. The slope of the linear line was taken as the pseudo-first-order rate constant ($k = 0.051$ min^{-1}).

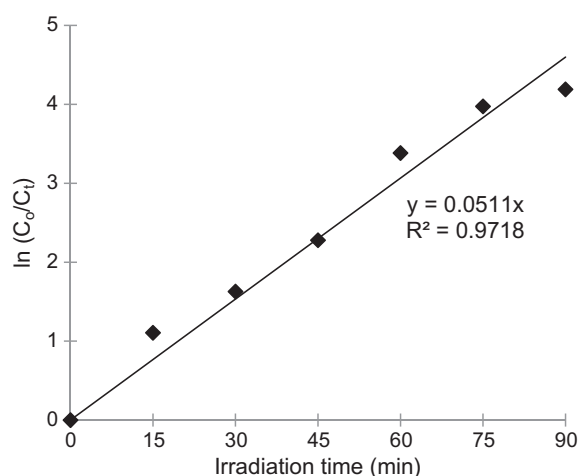Fig. 9. Plot of ln (C_0/C_t) vs. irradiation time.

4. Conclusion

In this work, a thin film of TiO_2 photocatalyst was successfully immobilized onto a glass support using a simple and fast dip coating technique in the presence of ENR solution as an adhesive agent. Household fluorescent lamp was chosen to be the visible light for the activation of TiO_2 film for decolorization of MB dye. The influence of TiO_2 loading, pH, and irradiation parameters on the photocatalytic decolorization efficiency process of MB was optimized using RSM. This factorial experimental design approach is a powerful tool, which can be used to develop empirical equation for the prediction and understanding of MB photocatalytic decolorization efficiency. As observed, the most effective parameters in the decolorization efficiency were pH and irradiation time. The interaction between pH and irradiation time was the most influencing interaction. However, the interaction between TiO_2 loading with pH and TiO_2 loading with irradiation time was the least influencing parameter.

Acknowledgments

References

[1] D. Pathania, S. Sharma, P. Singh, Removal of methylene blue by adsorption onto activated carbon developed from *Ficus carica* bast, Arab. J. Chem. http://dx.doi.org/10.1016/j.arabjc.2013.04.021.

[2] D. Ghosh, K.G. Bhattacharyya, Adsorption of methylene blue on kaolinite, Appl. Clay Sci. 20 (2002) 295–300.

[3] I.A.W. Tan, A.L. Ahmad, B.H. Hameed, Adsorption of basic dye on high-surface-area activated carbon prepared from coconut husk: Equilibrium, kinetic and thermodynamic studies, J. Hazard. Mater. 154 (2008) 337–346.

[4] D. Sannino, V. Vaiano, O. Sacco, P. Ciambelli, Mathematical modelling of photocatalytic degradation of methylene blue under visible light irradiation, J. Environ. Chem. Eng. 1 (2013) 56–60.

[5] H. Benaïssa, Influence of ionic strength on methylene blue removal by sorption from synthetic aqueous solution using almond peel as a sorbent material: Experimental and modelling studies, J. Taibah Univ. Sci. 4 (2010) 31–38.

[6] A. Vijayabalan, K. Selvam, R. Velmurugan, M. Swaminathan, Photocatalytic activity of surface fluorinated TiO_2-P25 in the degradation of reactive orange 4, J. Hazard. Mater. 172 (2009) 914–921.

[7] V.K. Gupta, R. Jain, A. Nayak, S. Agarwal, M. Shrivastava, Removal of the hazardous dye —Tartrazine by photodegradation on titanium dioxide surface, Mater. Sci. Eng.: C 31 (2011) 1062–1067.

[8] M.N. Chong, B. Jin, C.W.K. Chow, C. Saint, Recent developments in photocatalytic water treatment technology: A review, Water Res. 44 (2010) 2997–3027.

[9] M.A. Nawi, A.H. Jawad, S. Sabar, W.S.W. Ngah, Immobilized bilayer TiO_2/chitosan system for the removal of phenol under irradiation by a 45 watt compact fluorescent lamp, Desalination 280 (2011) 288–296.

[10] D.B. Hamal, K.J. Klabunde, Synthesis, characterization, and visible light activity of new nanoparticle photocatalysts based on silver, carbon, and sulfur-doped TiO_2, J. Colloid Interface Sci. 311 (2007) 514–522.

[11] Q. Zhang, W. Fan, L. Gao, Anatase TiO_2 nanoparticles immobilized on ZnO tetrapods as a highly efficient and easily recyclable photocatalyst, Appl. Catal., B 76 (2007) 168–173.

[12] L. Andronic, A. Duta, TiO_2 thin films for dyes photodegradation, Thin Solid Films 515 (2007) 6294–6297.

[13] P.W. Araúˊjo, R.G. Brereton, Experimental design II. Optimization, Trends Anal. Chem. 15 (1996) 63–70.

[14] T. Lundstedt, E. Seifert, L. Abramo, B. Thelin, Å. Nyström, J. Pettersen, R. Bergman, Experimental design and optimization, Chemom. Intell. Lab. Syst. 42 (1998) 3–40.

[15] J.H. Park, Treatment characteristics and statistical optimization of chloroform using sonophotocatalysis, Desalin. Water Treat. 51 (2013) 3106–3113.

[16] V. Mahmoodi, J. Sargolzaei, Optimization of photocatalytic degradation of naphthalene using nano-TiO_2/UV system: Statistical analysis by a response surface methodology, Desalin. Water Treat. (2014) 1–9, doi: 10.1080/19443994.2013.861774.

[17] J. Antony, R.K. Roy, Improving the process quality using statistical design of experiments: A case study, Qual. Assur. 6 (1999) 87–95.

[18] N. Barka, M. Abdennouri, A. Boussaoud, A. Galadi, M. Baâlala, M. Bensitel, A. Sahibed-Dine, K. Nohair, M. Sadiq, Full factorial experimental design applied to oxalic acid photocatalytic degradation in TiO_2 aqueous suspension, Arab. J. Chem. doi: 10.1016/j.arabjc.2010.12.015.

[19] A. Zuorro, M. Fidaleo, R. Lavecchia, Response surface methodology (RSM) analysis of photodegradation of sulfonated diazo dye Reactive Green 19 by UV/H_2O_2 process, J. Environ. Manage. 127 (2013) 28–35.

[20] A.H. Jawad, M.A. Nawi, Characterizations of the photocatalytically-oxidized cross-linked chitosan-glutaraldehyde and its application as a sub-layer in the TiO_2/CS-GLA bilayer photocatalyst system, J. Polym. Environ. 20 (2012) 817–829.

[21] R. Azargohar, A.K. Dalai, Production of activated carbon from Luscar char: Experimental and modeling studies, Micropor. Mesopor. Mater. 85 (2005) 219–225.

[22] A. Hassani, L. Alidokht, A.R. Khataee, S. Karaca, Optimization of comparative removal of two structurally different basic dyes using coal as a low-cost and available adsorbent, J. Taiwan Inst. Chem. Eng. 45 (2014) 1597–1607.

[23] A.R. Khataee, M.B. Kasiri, L. Alidokht, Application of response surface methodology in the optimization of

photocatalytic removal of environmental pollutants using nanocatalysts, Environ. Technol. 32 (2011) 1669–1684.

[24] D. Baş, I.H. Boyacı, Modeling and optimization I: Usability of response surface methodology, J. Food Eng. 78 (2007) 836–845.

[25] L. Alidokht, A.R. Khataee, A. Reyhanitabar, S. Oustan, Cr(VI) immobilization process in a Cr-spiked soil by zerovalent iron nanoparticles: Optimization using response surface methodology, CLEAN—Soil Air Water 39 (2011) 633–640.

[26] M.J. Anderson, P.J. Whitcomb, RSM Simplified: Optimizing Processes Using Response Surface Methods for Design of Experiments, Productivity Press, New York, NY, 2005.

[27] A.H. Jawad, M.A. Nawi, Fabrication, optimization and application of an immobilized layer-by-layer TiO_2/chitosan system for the removal of phenol and its intermediates under 45-W fluorescent lamp, React. Kinet. Mech. Cat. 106 (2012) 49–65.

[28] U.I. Gaya, A.H. Abdullah, Heterogeneous photocatalytic degradation of organic contaminants over titanium dioxide: A review of fundamentals, progress and problems, J. Photochem. Photobiol., C 9 (2008) 1–12.

[29] K. Elghniji, M. Ksibi, E. Elaloui, Sol–gel reverse micelle preparation and characterization of N-doped TiO_2: Efficient photocatalytic degradation of methylene blue in water under visible light, J. Ind. Eng. Chem. 18 (2012) 178–182.